http://dx.doi.org/10.21611/qirt.2014.214

Infrared thermography to evaluate impact damaging of thermoplastic composites

by S. Boccardi[1], G.M. Carlomagno[1], C. Meola[1], P. Russo[2] and G. Simeoli[3]

[1]Department of Industrial Engineering-Aerospace Division, University of Naples Federico II, Via Claudio 21- 80125 Napoli, Italy

[2]Institute for Polymers, Composites and Biomaterials, National Council of Research, via Campi Flegrei 34, 80078 Pozzuoli (Na), Italy

[3]Department of Chemical, Materials and Production Engineering, University of Naples Federico II, P.le V. Tecchio 80- 80125 Napoli, Italy

Abstract

Infrared thermography (IRT) is used to get information on the behavior of thermoplastic matrix composites under low velocity/energy impact. Indeed, infrared thermography proved already its usefulness in the investigation of impact damaging of composites, as both surface thermal mapping when the specimen is being impacted and non destructive evaluation technique. However in the past, IRT has been mainly used with thermoset matrix composites, while the attention of the present work is focused on composites with a thermoplastic matrix. Several specimens are considered involving two types of matrix: pure polypropylene and a modified one with addition of a compatibilizing agent based on maleic anhydride. A quite different behaviour is found for thermoplastic composites with respect to thermoset ones in terms of both the reaction to the impact event and the occurred damage. Besides at high impact energy values, the behaviour of the two types of matrices is completely different.

1. Introduction

Composite materials are ever more increasingly used in many industrial applications. Their success is mainly due to their high strength-to-weight ratio, formability, and other properties that may make them preferable to metals and other conventional engineering materials. At first, the development of composites was driven by the aircraft requirements leading mainly to the use of thermoset polymers as matrix, because of their low density (low weight). The main weakness of all the fibre reinforced thermoset polymers is their relatively low interlaminar strength, which makes them susceptible to delamination under impact load [1]. Recently, the introduction of composites in other transport sectors, like the automotive, naval and railway, where the lightness is not a commitment as in airplanes, has extended the research interest towards the development and use of thermoplastic matrix composites.

Actually, to maximize the composite toughness, thermoplastic matrices are the most promising ones; in fact, they are characterized by higher damage tolerance and interlaminar toughness, with an intrinsic structure able to limit the crack propagation process and allow larger deformations [2], so as to make the material more resilient. Thermoplastic matrices also display advantages over the thermoset ones in terms of potential recyclability after the life-cycle, reprocessing, chemical and environmental resistance, reduced moisture absorption and, usually, faster as well as reduced cost production processes [3]. Among the thermoplastic matrices, polypropylene (PP) is considered one of the most promising because of its low density, good processability and environmental resistance. In addition, a good-to-impact performance material can be tailored by managing the fibers/matrix interfacial strength. In fact, as recently shown by Russo et al. [4] for thermoplastic composites based on PP and glass fiber reinforcement, the interfacial strength between fibers and matrix plays a key role in dissipating energy during an impact.

The attention of the present work is devoted towards the understanding of the behavior to low velocity/energy impact loads of polypropylene based laminates reinforced with glass fibres and with a change of interfacial strength. Infrared thermography proved already its usefulness to get information about impact damaging of thermoset matrix composites. It was used with a two-fold objective of surface thermal mapping when the specimen is being impacted and as non destructive evaluation (NDE) technique after impact [5-7]. In particular, Meola and Carlomagno supplied information on the onset and propagation of impact damage in Glass Fibres Reinforced Polymers (GFRP) through the analysis of thermoplastics effects [5]. More recently, they demonstrated the important role played by manufacturing defects, like porosity and fibres misalignment, in the behaviour of GFRP to impact load [7]. Infrared thermography proved also suitability to establish the impact energy value for onset of Carbon Fibres Reinforced Polymers (CFRP) material damage in agreement with the acoustic emission recorded by piezo patches [6].

It is worth noting that in all the previous works [5-7] the material matrix was a thermoset one, while presently the attention is focused on materials with a thermoplastic matrix. More specifically, the purpose is to use infrared thermography to get information about the behaviour, under impact load, of a thermoplastic matrix reinforced with glass fibres. To this end several specimens are fabricated by considering two types of matrix: a pure polypropylene and a modified one with addition of a compatibilizing agent based on maleic anhydride. Different tests are carried out using

http://dx.doi.org/10.21611/qirt.2014.214

either a falling dart machine, or a modified Charpy pendulum, all impacted specimens being inspected with lockin thermography to account for the impact damage occurred. The infrared imaging system is also used to monitor the impact phase generated by the Charpy pendulum.

2. Description of materials and tests

Two polypropylene based composites laminates reinforced with woven glass fabrics are produced by film stacking technology with different fibre/matrix interface strength. In this regard, composite systems involve a film grade PP matrix (MA712 from Unipetrol – Czech Republic with MFI = 12g/10 min), pure or modified by previous addition of 2% by weight of polypropylene grafted maleic anhydride (PP-g-MA) commercialized under the trade name of Polybond 3200 (MFI = 115g/10min, 1wt% maleic anhydride, from Chemtura). In this way, two types of composite specimens, in the following coded as P and C, respectively, are fabricated and analyzed.

Each specimen includes 20 balanced glass fabric layers 0°/90° symmetrically arranged with respect to the middle plane of the laminate ($[(0/90)_{10}]_s$ configuration), with a target thickness of 3 mm and a glass fibre content of 50% by volume as evaluated according to ASTM D 3171-99. Films of either pure, or compatibilized polypropylene are prepared with the film blowing extrusion line model Teach-Line E 20 T (Collin Gmbh, Germany); the final thickness varying between 35 and 40 µm. Then composite laminates are obtained by alternating layers of polypropylene films and glass fibre fabrics by the hand lay-up film-stacking technique. Composite specimens are obtained from laminates produced by using a compression moulding machine (model P300P, Collin Gmbh, Germany) according to a pre-optimized moulding cycle.

Then, all the specimens are subjected to low velocity/energy impact tests by using either a falling dart machine (model Fractovis Plus, Ceast, Italy), or a modified Charpy pendulum. In both cases, the impactor has a 12.7 mm hemispheric tip. The impact energy is varied between 5 and 20 J. In the falling dart machine, the specimen is housed between two rings of 40 mm (60 mm) inner (outer) diameter. Impact tests are also performed with a modified Charpy pendulum which allows enough room for positioning of the infrared camera to view the rear specimen surface (i.e., opposite to that struck by the hammer) [5-7]. Specimens are placed inside a special lodge which includes two larger plates, each with a window 150 mm x 75 mm to allow for the contact with the hammer from one side and optical view (by the infrared camera) from the other side. The impact energy E is set by suitably adjusting the falling height of the Charpy arm. Sequences of thermal images are acquired at 96 Hz during impact tests. To allow for a complete visualization of thermal effects evolution with respect to the ambient temperature, the acquisition starts few seconds before the impact and lasts for some time after.

All specimens are non-destructively evaluated with lockin thermography to get information about the impact damage extension. The used infrared camera is the SC6000 (Flir systems), which is equipped with a QWIP detector, working in the 8-9 µm infrared band, NEDT < 35mK, spatial resolution 640x512 pixels full frame with the pixel size 25 µm x 25 µm and with a windowing option linked to frequency frame rate and temperature range. The camera is equipped with the Lockin option and the IRLockIn© software for performing lockin thermography tests.

3. Non-destructive evaluation

The specimens impacted with the falling dart machine are only non-destructively evaluated with lockin thermography. The test setup includes the specimen, the infrared camera and a halogen lamp for thermal stimulation of the specimen itself [5]. More specifically, the infrared camera is equipped with a Lock-in module that drives the halogen lamp to generate a thermal wave of selectable frequency f. The thermal wave, delivered to the specimen surface, propagates inside the material and gets reflected when it reaches parts where the heat propagation parameters change (in-homogeneities). The reflected wave interferes with the surface wave producing an oscillating interference pattern, which can be measured in terms of either temperature amplitude or phase angle ϕ, and represented as amplitude, or phase, images, respectively. The basic link of the thermal diffusion length μ to the heating frequency f and to the material thermal diffusivity coefficient α is via the relationship:

$$\mu = \sqrt{\frac{\alpha}{\pi f}} \qquad (1)$$

The depth range for the amplitude image is given by μ, while the maximum depth p, which can be reached for the phase image, corresponds to 1.8 μ [8-10]. In general, it is preferable to reduce data in terms of phase image because of its insensitivity to both non uniform heating and local variations of emissivity over the monitored surface. The material thickness, which can be inspected, depends on the wave period (the longer the period, the deeper the penetration) and on the material thermal diffusivity.

According to Eq.1, the knowledge of the thermal diffusivity is fundamental to evaluate the depth at which any detected anomaly is located, or to chose the frequency value to check the material conditions at a given depth. To this end, the thermal diffusivity α (Eq.1) is evaluated with the lockin technique itself; the procedure is described in a previous work by Meola et al. [11]. For the intact (not impacted) materials, it was found a value of α = 0.013 cm^2/s for the P type and α = 0.017 cm^2/s for the C type specimens. Impact may modify these values.

http://dx.doi.org/10.21611/qirt.2014.214

A comparison between phase images taken from both sides of specimens type P impacted with the falling dart machine is made in Fig.1. As it can be seen, while the phase images taken from the impacted side (Fig.1a) clearly depict the occurred damage, those taken from the opposite side (Fig.1b) are less revealing being also affected by reflections over the conical protrusion. In fact, thermoplastic matrix composites react to the impact with visible modifications, like metals, displaying an indentation (a small concavity) on the impacted side and a protrusion on the rear one. Of course, these modifications are very slight for very low impact energy, while they become ever more pronounced by increasing the impact energy. In particular, the base of the conical protrusion (Fig.1b) is encircled by the sample holder ring indentation (circular dark stripe). Given that, in practical applications, only the external impacted surface is available, in the following only phase images taken from the impacted side will be shown.

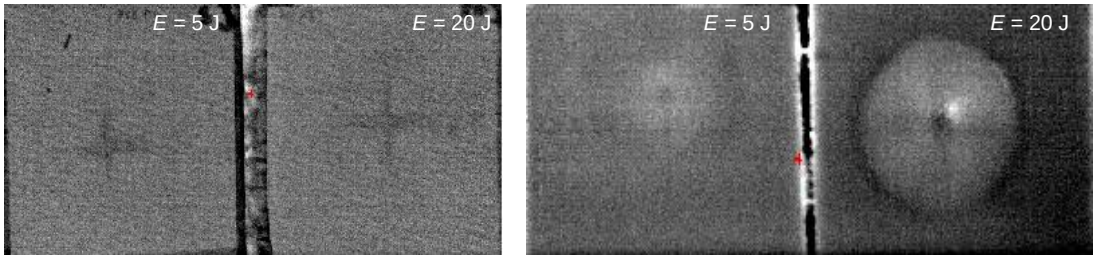

a) Impacted side b) Rear side

Fig. 1. *Phase images of specimens type P impacted with the falling dart machine.*

The following figures 2 and 3 show phase images taken at different heating frequencies *f*, ranging from 0.15 to 0.53 Hz for both P (Fig.2) and C (Fig.3) types of specimens, which are impacted with the falling dart machine at two impact energies *E* = 5 J and 20 J. The *f* values are chosen so as to look for the material conditions at different depth *p* through the thickness (see Table 1).

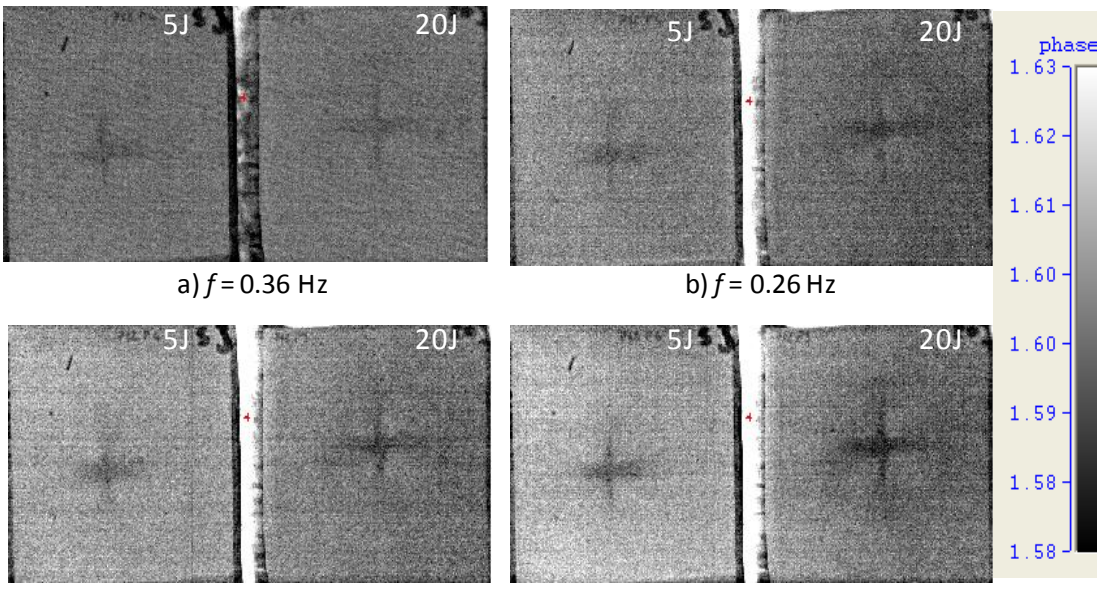

a) *f* = 0.36 Hz b) *f* = 0.26 Hz

c) *f* = 0.19 Hz d) *f* = 0.15 Hz

Fig. 2. *Phase images, taken for varying the heating frequency, of specimens type P impacted with the falling dart machine.*

As can be seen, the P type specimens show some damage (darker zones) already at the lowest impact energy of 5 J and at the high *f* value (Fig. 2a). In particular, the damage over the pure polypropylene matrix specimen takes the classical cross shaped appearance, which is quite similar to that observed on the thermoset matrix based materials for 0°/90° fabric laminates [6]. Such a cross pattern is still present over the P type specimen impacted at the greater energy of 20 J, but, of course, with longer sides to account for an increased damage extension. In addition, for *E* = 20 J a darker circle can also be distinguished for *f* = 0.26 Hz (Fig.2b) which becomes more evident to a further *f* reduction; such a dark circle indicates the local material modifications induced by the indentation of the specimen holder ring.

The C type specimens (Fig.3) display a quite different behaviour from the previous one and with varying the impact energy. In fact for *E* = 5 J and *f* = 0.53 Hz, it is hard to distinguish any indentation sign (Fig.3a left) while, with

http://dx.doi.org/10.21611/qirt.2014.214

decreasing f, a dark oblong zone appears accounting for some damage there. Instead, for E = 20 J, a small lighter disc is present (Fig.3a right) for f = 0.53 Hz accounting for surface indentation. As f decreases, darker ray beams appear around the white disc, which in the meantime becomes oblong and intensifies in contrast (Fig.3c, d). This indicates fibres breakage in the centre (practically nearby the tip of the protrusion cone that is present on the rear side) with delaminations moving in a sunburst fashion. No sign of the sample holder ring is present. Indeed, for C type specimens, the strong interfacial strength is responsible for the failure of fibres, since it cannot tolerate large deformations, unlike the not compatibilized matrix based samples of type P.

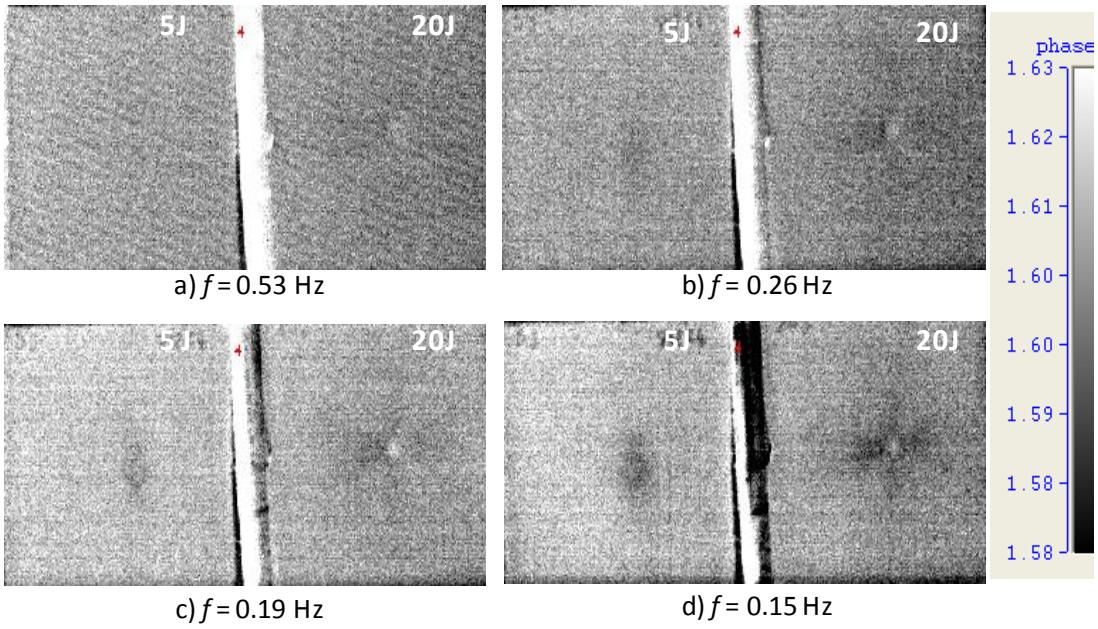

Fig. 3. *Phase images, taken for varying the heating frequency, of specimens type C impacted with the falling dart machine.*

Table 1. *Depth values at different heating frequencies for the two specimens types*

f [Hz]	p [mm]	
	P	C
0.53	1.59	1.82
0.36	1.90	2.20
0.26	2.20	2.59
0.19	2.65	3.00
0.15	2.98	3.40

Fig. 4 shows phase images taken at the heating frequency of f = 0.15 Hz of P (Fig.4a) and C (Fig.4b) types specimens, which were both impacted with the Charpy pendulum at two impact energies E = 5 J and 20 J. It is worth noting that Fig.4 shows phase images, taken at the same heating frequency for both specimens' types in the light of a general comparison. However, as determined with the same lockin thermography technique, the presence of the compatibilizing agent affects, to a certain extent, the material thermal diffusivity.

By comparing Fig.4 to Figs.2 and 3, it is possible to see that the different material response to the impact is retained, but some differences may be recognized which are to be ascribed partly to the impacting apparatus but mainly to the different sample holders. In particular, owing to the phase images taken on the type C specimens, it seems that the damage caused by the Charpy pendulum (Fig.4b) extends over a smaller area with respect to that caused by the falling dart machine (Fig.3).

This effect can be verified by looking at Fig.5 which shows photos taken from both sides of specimens impacted at E = 20 J with either the falling dart machine (Fig.5a, b), or the Charpy pendulum (Fig.5c, d). In fact, a higher protrusion cone as well cuts in horizontal and vertical directions are visible in Fig.5b accounting for the larger damage caused by the falling dart machine. It is just the breakage at the tip of the protrusion (Fig.5b) that appears as whiter zone in the phase images of Fig.3c and d (remember that the phase images are taken from the impacted side); in addition, the protrusion cone on the rear gives rise to the sunburst effect in the phase image. Analogously, Fig.5d is in agreement with Fig.4b (right), displaying both damage along three horizontal fibres.

http://dx.doi.org/10.21611/qirt.2014.214

It seems that lockin thermography is able to detect any modification induced by the impact in any type of material, but a question may arise: What really happens during an impact event? A help to provide an answer to this query is supplied by an infrared camera used to monitor the impact event while is occurring.

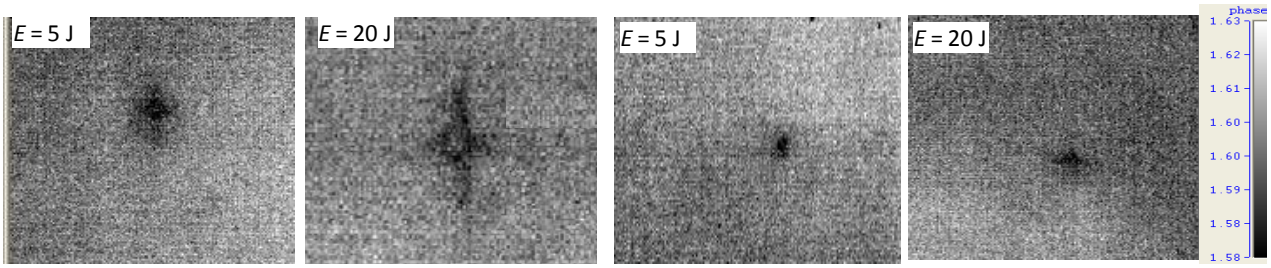

a) P type specimens b) C type specimens

Fig. 4. *Phase images, taken at the heating frequency f = 0.15 Hz, of P (a) and C (b) types specimens impacted with the Charpy pendulum*

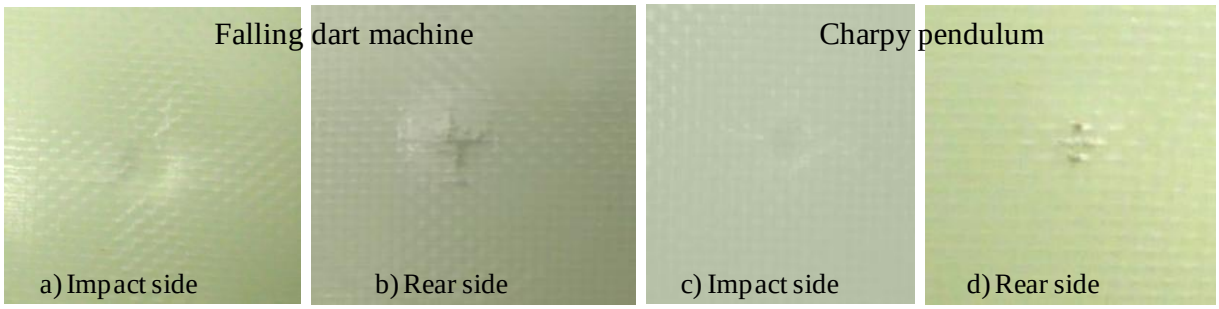

Fig. 5. *Photos taken from both sides of specimens C after impact at E = 20 J with a falling dart machine (a) and a Charpy pendulum (b)*

4. Impact monitoring

Some impact tests are performed with the Charpy pendulum that allows positioning of the infrared camera to monitor the thermal effects developing on the specimen surface opposite to the impact. Sequences of thermal images are acquired at a frame rate of 96 Hz during impact tests. To allow for a complete visualization of thermal effects evolution with respect to the ambient temperature, the acquisition starts few seconds before the impact and lasts for some time after. In order to better analyse the material's thermal behaviour, the first image (t = 0 s) of the sequence, i.e. the specimen surface (ambient) temperature before the impact, is subtracted to each subsequent image so as to generate a map of temperature difference ΔT:

$$\Delta T = T(i,j,t) - T(i,j,0) \qquad (2)$$

i and *j* representing lines and columns of the surface temperature array.

Some ΔT images, taken 0.656 s after the first impact sign (as detected by the infrared camera), with the impact energy varying in the range E = 5 ÷ 20 J, of both types of specimens are shown in the following figures 6 and 7. To facilitate a comparison, all the images are presented with the same ΔT scale (-0.2 ÷ 1.5). However, this scale is appropriate for the P type specimens at any of the investigated impact energies (Fig.6), while it is not suitable to cover the temperature variations undergone by the type C specimens (Fig.7) at the different impact energies. In fact, an increase in temperature enough above ΔT = 1.5 is reached for E = 20 J (Fig.7d). Thus, the image of Fig.7d is shown again in Fig.8b with a more appropriate scale, together with an earlier image (Fig.8a).

As can be seen, Fig.6a, which is relative to E = 5 J, displays a central small darker zone surrounded by a lighter corona. This corona first strengthens up for increasing the impact energy to 10 J and after it becomes much milder to a further increase of the impact energy. To better account for the temperature evolution during the impact event, ΔT values in two points, specifically in the central darker zone (P_{in}) and over the lighter corona (P_{out}), are plotted versus the number of frames in Fig. 9 for E = 5 J (Fig. 9a) and 20 J (Fig. 9b), respectively. The ΔT distribution displays in both P_{in} and P_{out} a value equal to zero before the impact, when the specimen surface is at ambient temperature, a sudden decrease below zero at the impact, followed by an equally rapid rise. More specifically, the temperature after the sudden jump continues to increase slowly toward a maximum value which remains almost constant for quite long time.

http://dx.doi.org/10.21611/qirt.2014.214

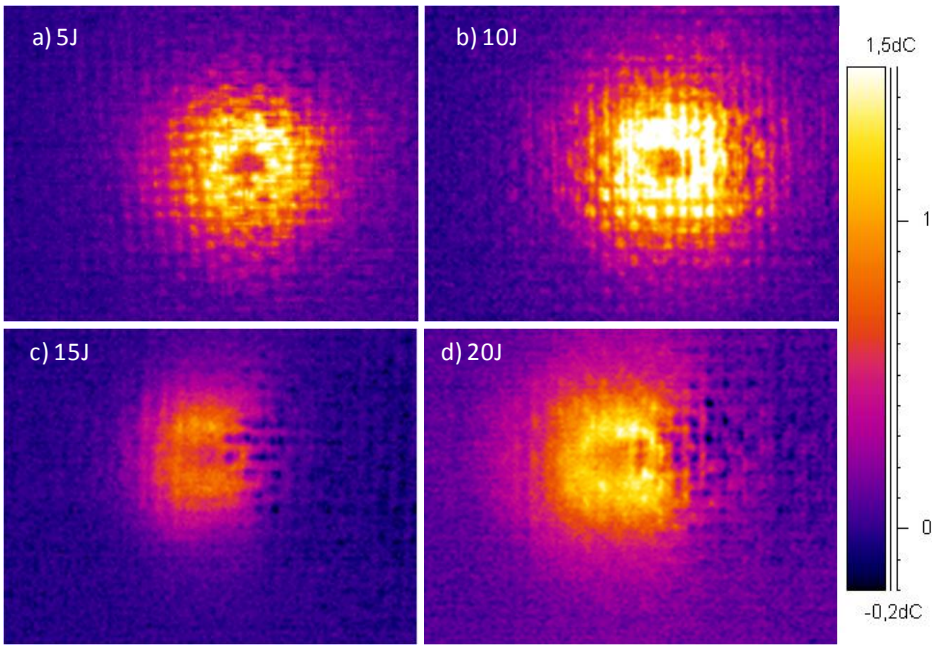

Fig. 6. *Thermal images taken 0.656 s after the impact on type P specimens*

The negative ΔT values which initially appear in all the diagrams of Fig.9 are due to thermo-elastic effects because the impact load causes bending of the material with consequent cooling down on the opposite side where the material is under traction; of course, the higher is the impact energy, the larger the bending and the lower the reached temperature value.

Conversely, the maximum ΔT in the outer corona of Figs. 6 and 7 may indicate dissipation of the impact energy through material delamination; it seems to be slightly affected by the impact energy (Fig.9a, b) at least till E = 20 J. The main difference, to a comparison between Fig.9a and Fig.9b, consists in the higher rise of temperature in P_{in} for E = 20 J (Fig.9b) which leads to a more quick uniformity of P_{in} and P_{out} temperatures. In Fig.9a-c, while the continuous temperature increase with time of P_{in} is certainly due to the warmer surrounding zone, the initial increase with time of P_{out} is most probably due to the presence of nearby warmer zones.

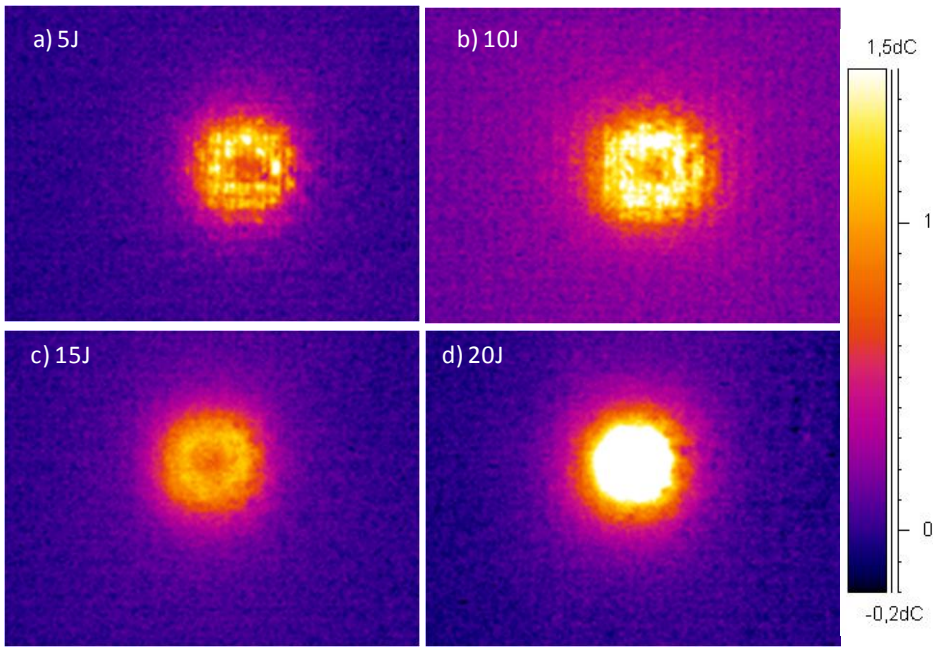

Fig. 7. *Thermal images taken 0.656 s after the impact on type C specimens*

http://dx.doi.org/10.21611/qirt.2014.214

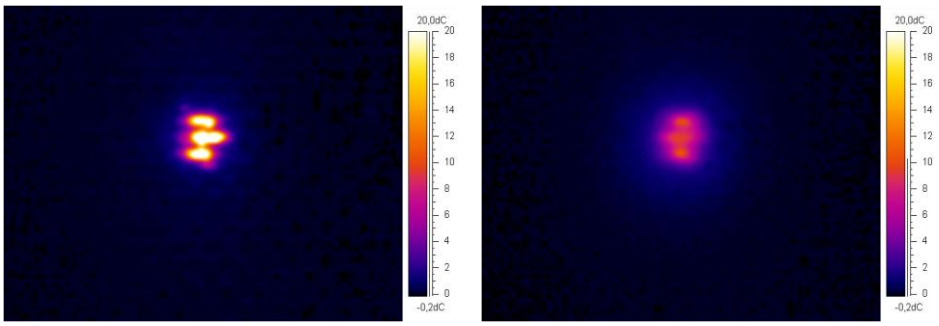

a) t = 0.135 s b) t = 0.656 s

Fig. 8. *Thermal images of type C specimen impacted at E = 20 J (the same specimen of Fig.7d)*

Owing to the type C specimens, it is possible to see that for E in the range 5 ÷ 15 J (Fig.7 and Fig.9c) the material behaves in a way similar to the type P specimens. The only difference is the smaller diameter of the thermal signature, which is easily noticeable from a comparison between Figs. 6 and 7 (note that the spatial resolution is the same). Indeed, such a reduction of the damaged area for specimens type C was already evidenced in Section 3 while comparing Fig.2 to Fig.3 even if those specimens were impacted with the falling dart machine.

Instead, for E = 20 J, the type C specimen displays a strong overheating (Fig. 7d) being the image in saturation. To better investigate this occurrence, the scale is adjusted in Fig.8b and another image at a previous instant (t = 0.135 s) is also shown (Fig.8a). As can be seen, three horizontal oblong hot zones, involving three fibres pockets, are clearly distinguishable. In particular, as shown in the plots in Fig.9d, they are interested by an abrupt temperature rise, which in the central zone reaches values above 30 K (Fig.9d). Then, the temperature decreases first rapidly and after more slowly (driven by the ΔT value) towards a value of about 2 K that remains almost constant for a relatively long time. Owing to previous observations on thermoset matrix based materials [5, 7], this overheating indicates a large dissipation of impact energy involving local fibres breakage; this occurrence is also visible to the naked eye (Fig. 5d). From a comparison of Fig. 9d to Fig. 9b it can be stressed once more, the different behaviour of the two material types (P and C) meaning that the presence of the compatibilizing agent in the matrix prevents large deformations in the impact zone, favouring local breakage.

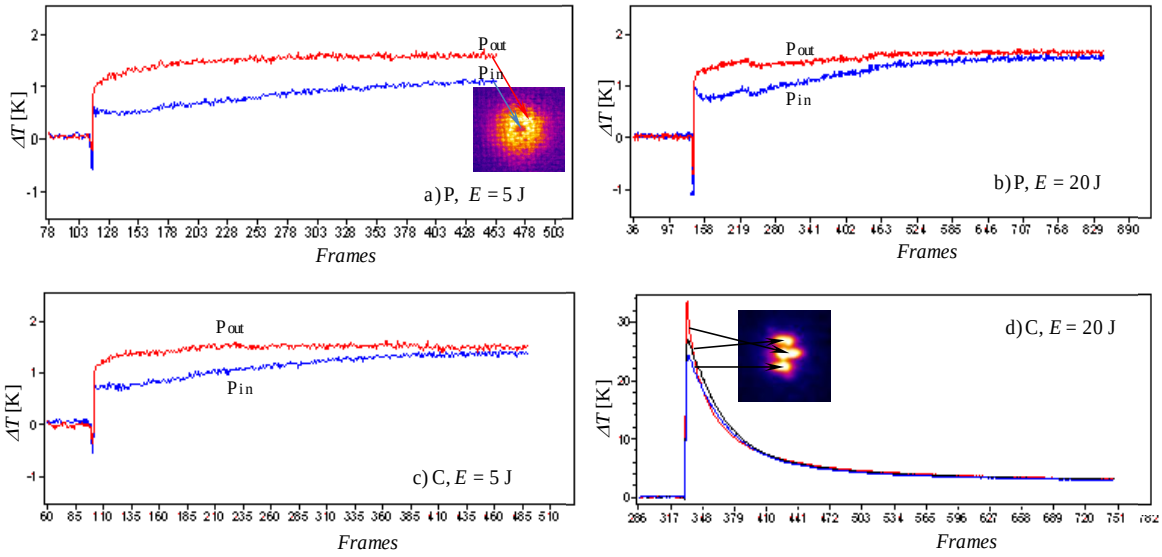

Fig. 9. *ΔT distribution on some specimen spots*

From Figs. 6 and 7 it is also possible to evaluate the warm area A_W which helps to quickly get information about the extension of the damaged area. Owing to the change of colour (ΔT value*)* with respect to the background (sound material), it is easy to see that for the type P specimens (Fig. 6) A_W first increases with increasing E from 5 to 10 J, then it slightly decreases for E = 15 J and after it increases again for E = 20 J. This phenomenon may be due to a combined effect of material plastic deformation and thickness variation which depends on the impact energy.

For the type C specimens (Fig. 7) A_W is, on the overall, smaller with respect to the type C specimens and practically coincides with the size of the impactor nose for every impact energy. Thus, it could be inferred that deformations in a compatibilized polypropylene matrix are restricted to the size of the pushing element.

http://dx.doi.org/10.21611/qirt.2014.214

5. Conclusions

Infrared thermography has been used to either detect the damage caused by low energy impacts, or to monitor the impact event, within two types of materials involving glass fibres embedded in a thermoplastic matrix, with and without a compatibilizing agent. In general, a quite different behaviour is found for thermoplastic composites with respect to thermoset ones in terms of both the impact event and the occurred damage. Besides, it is possible to distinguish the different damaging ways of the two matrix materials. In fact, specimens involving a compatibilizing agent in the polypropylene matrix react to the impact with a plastic deformation limited to the size of the impactor nose, which is smaller than the deformation undergone by a pure polypropylene matrix at the same impact energy. Furthermore, due to the more limited deformation of the modified matrix, the highest impact energy (20J) is dissipated within a small area with fibers breakage.

REFERENCES

[1] Abrate S., Impact on composite structures. Cambridge: Cambridge University Press, 1998.
[2] Çoban O., Bora M.Ö., Sinmazçelik T., Cürgül İ., Günay V., “Fracture morphology and deformation characteristics of repeatedly impacted thermoplastic matrix composites”, Materials & Design, vol. 30, pp. 628–34, 2009.
[3] Collier M.C., Baird D.G., “Separation of a thermotropic liquid crystalline polymer from polypropylene composites”, Polymer Composites, vol. 20,pp. 423–35, 1999.
[4] Russo P., Acierno D., Simeoli G., Iannace S., Sorrentino L., “Flexural and impact response of woven glass fiber fabric/polypropylene composites”, Composites Part B: Engineering, vol. 54, pp. 415–21, 2013.
[5] Meola C., Carlomagno G.M., “Impact damage in GFRP: new insights with Infrared Thermography”, Composites Part A, vol.41, pp. 1839-1847, 2010.
[6] Meola C., Carlomagno G.M., Ricci F., “Monitoring of impact damage in Carbon Fibre Reinforced Polymers”, QIRT 2012, Napoli, June 11-14, 2012, paper n. 374, pp.8.
[7] Meola C., Carlomagno G.M., “Infrared thermography to evaluate impact damage in glass/epoxy with manufacturing defects”, International Journal of Impact Engineering, (67), 1-11, 2014.
[8] Letho A., Jaarinen J., Tiusanen T., Jokinen M., Luukkala M., “Magnitude and phase in thermal wave imaging”, Electron. Lett. (17), 364–365, 1981.
[9] Bennett C. A. Jr., Patty R. R., “Thermal wave interferometry: a potential application of the photoacoustic effect”, Appl. Opt. (21), 49–54, 1982.
[10] Busse G., “Optoacoustic phase angle measurement for probing a metal”, Appl. Phys. Lett. (35), 759–760, 1979.
[11] Meola C., Carlomagno G.M., Squillace A., Giorleo G., “Non-destructive control of industrial materials by means of lock-in thermography”, Meas. Sci. Technol., 13 (2002), 1583-1590.